Radiological evaluation of industrial residues for construction purposes correlated with their chemical properties

Peer-reviewed author version

SAS, Zoltan; VANDEVENNE, Niels; Doherty, Rory; Vinai, Raffaele; Kwasny, Jacek; Russell, Mark; Sha, Wei; Soutsos, Marios & SCHROEYERS, Wouter (2019)
Radiological evaluation of industrial residues for construction purposes correlated with their chemical properties. In: Science of the total environment, 658, p. 141-151.

DOI: 10.1016/j.scitotenv.2018.12.043
Handle: http://hdl.handle.net/1942/27647

Radiological evaluation of industrial residues for construction purposes correlated with their chemical properties

Zoltan Sas[1,2], Niels Vandevenne[2], Rory Doherty[1], Raffaele Vinai[3], Jacek Kwasny[1], Mark Russell[1], Wei Sha[1*], Marios Soutsos[1], Wouter Schroeyers[2]

[1]*School of Natural and Built Environment, Queen's University Belfast, David Keir Bldg., 39-123 Stranmillis Rd, Belfast BT9 5AG, United Kingdom*

[2]*Hasselt University, CMK, Nuclear Technological Centre (NuTeC), Faculty of Engineering Technology, Agoralaan, Gebouw H, 3590 Diepenbeek, Belgium*

[3]*College of Engineering, Mathematics and Physical Sciences, Harrison Bldg., University of Exeter, North Park Road, Exeter EX4 4QF, United Kingdom*

**Corresponding author: w.sha@qub.ac.uk*

Abstract

This study characterises the naturally occurring radionuclide (NOR) contents of a suite of secondary raw materials or industrial residues that are normally disposed of in landfills or lagoons but now are increasingly used in green concretes. This includes ashes from a variety of industrial processes and red mud from aluminium production, as well as air pollution control residue and cement kiln dust. The chemical composition of the samples was determined with X-ray fluorescence spectroscopy (XRF). The Ra-226, Th-232 and K-40 activity concentrations were obtained by gamma spectrometry, and the results were compared with recently published NOR databases. The correlation between the NOR contents and the main chemical

composition was investigated. The radioactive equilibrium in the U-238 chain was studied based on the determination of progeny isotopes. The most commonly used calculation methods (activity concentration index and radium equivalent concentration) were applied to classify the samples. The radon exhalation rate of the samples was measured, and the radon emanation coefficient was calculated. Significant correlation was found between the NORs and certain chemical components. The massic exhalation demonstrated a broad range, and it was found that the emanation coefficients were significantly lower in the case of the residues generated as a result of high-temperature combustion processes. The results showed a weak correlation between the Ra-226 concentration and the radon exhalation. This emphasizes that managing the Ra-226 content of recycled material by itself is not sufficient to control the radon exhalation of recycled materials used in building products. The investigated parameters and their correlation behaviour could be used to source apportion materials found during the process of landfill mining and recovery of material for recycling.

Keywords: gamma spectrometry; radon emanation; radon exhalation; recycling; red mud

Highlights

- The NOR contents of the surveyed residues fit well with recent NOR databases
- The radioactive equilibrium in the decay chains fits well with the literature data
- Strong correlation was found between the NOR contents and certain chemical elements
- The chemical composition can be used as a source apportionment tool for NOR content
- The emanation was low for residues generated under high-temperature processes

1. Introduction

The depletion of raw materials and demand for low carbon material resources has resulted in the urgent need for new eco-innovative building materials. The market need for efficient, economical and safe production of new building products requires a comprehensive model of the properties of primary and secondary raw materials, and existing building products to facilitate the creation of a circular economy. *"The transition to a more circular economy, where the value of products, materials and resources is maintained in the economy for as long as possible, and the generation of waste minimised, is an essential contribution to the EU's efforts to develop a sustainable, low carbon, resource efficient and competitive economy*" (European Commission, 2015). These material resources are often recycled from secondary raw materials or industrial residues rather than from pristine sources. Valorisation alongside carbon capture technologies can offer an opportunity for a circular economy approach to building materials (Pan et al., 2018). Alkali-activated materials (AAMs) are alternative low-carbon binders and can be produced through the reuse of industrial residues as secondary raw materials. These residues have traditionally been disposed of in brownfield landfills and lagoons which are now being mined to recover the valuable materials.

These residues often serve as precursors for production of AAM. Ideally the activators should be also residues or secondary raw materials with high pH (Tong et al., 2018). Here we focus on the residues that can be used in the production of AAMs. Globally, about 46% of CO_2 emissions originated as a result of the fossil fuel combustion, with 31% emitted from coal combustion power plants (Olivier et al., 2016). The amount of generated residue depends on the non-combustible mineral content, which can vary between 5-30% (Kovacs et al., 2017). As a result of combustion, the NOR contents of the coal are enriched in the residues (Table 1). A tenfold enrichment factor, compared to the initial NOR contents of the coal, is common in residues (Somlai et al., 1996). Owing to this phenomenon, residues, including the coarse bottom ash (BA), also called coal slag, and the fine, fly ash (FA), contain elevated (Kovacs et al., 2017; Kardos et al., 2015) and occasionally extremely high concentrations of Ra-226 (Somlai et al., 2006; Somlai et al., 1996) above the 1000 Bq/kg clearance level defined in the EU BSS (European Union, 2014). The use of BA and

FA in construction materials always increases the risk to residents. The iron production process produces slag as a residue. The NOR contents of the ground granulated blast-furnace slag (GGBFS) (Table 1) depend on the materials used during the process such as iron ore, sinter, flux limestone, dolomite, and coke. Aluminium production from bauxite produces red mud. The red mud still contains valuable compounds. Huge efforts are made to find economical technology to valorise them. However, when reused on an industrial scale it will still be subject to an 'end of waste criteria' depending on the country where this occurs. Globally, this is estimated at 150 million tons per year (Davris et al., 2015). The safe reuse of red mud has not been resolved yet, due to its heavy metal and its elevated NOR contents (Table 1). The unsafe storage of the red mud can endanger eco-systems and humans, as was demonstrated by disasters that happened in 2010 at Ajka, Hungary (Somlai et al., 2010; Gelencsér et al., 2011; Mayes et al., 2016) and in 2016 at Luoyang, Henan province, China, the latter fortunately without human injury (Liu, 2016). Red mud needs to be checked for its NOR contents when it is used in building materials (Kovacs et al., 2017). Cement kiln dust (CKD) presents a significant landfill and disposal problem (Gunning et al., 2010). There was no information found in the current literature regarding the NOR contents of the CKD. However, for comparison, cement data can be used as a proxy with the assumption that the CKD generated from the same stream as cement production is composed of the same unreacted raw material (US EPA, 2016). Municipal residue, clinical residue and sewage sludge produce signifcant amounts of ash (Rani et al., 2008). The ash, e.g. household waste ash (HWA), incinerated sewage sludge ash (ISSA) and dust, e.g. air pollution control (APC) residue, originate as a result of the scrubbing of emissions, with the residue often classified as hazardous (Kourti et al., 2010; Rani et al., 2008). Numerous studies have dealt with their reuse in the cement and concrete industry (Cyr et al., 2007; Donatello and Cheeseman, 2013; Wongsa et al., 2017; Müller and Rübner, 2006). As a result of the incineration, the radionuclides mainly remain in the solid residues (Carvalho, 2017). A study performed in Germany (Puch et al., 2005) measured the NOR contents of the HWA and compared them with the world averages published in RP-112 (European Commission, 1999). The radionuclide contents of ISSA mainly depend on the treated wastewater. The NORs and also artificial radionuclides, most notably I-131, Tl-201, and Sr-89 (all short half-lived medical isotopes), can accumulate

in the sludge and after the incineration remain in the inert inorganic particles of the ISSA. A survey, involving 313 Publicly Owned Treatment Works across the USA, concluded that elevated levels of radioactive materials were found in some sewage sludge and ash samples, but the survey did not indicate a widespread problem (ISCORS, 2005). Rice kusk ash (RHA), a residue of biomass-based electricity generation, originates from rice mills. The husk consists of approximately 40% cellulose, 30% lignin and 20% silica and is burned in power plants producing a residue with a hard, abrasive nature. The high silica content (~90-95%) and the reactive nature of the amorphous silica content makes it usable as a pozzolana (He et al., 2013). Information in the scientific literature about the NOR contents in RHA is currently missing.

This circular approach requires cross-disciplinary collaboration between academics, industry, and the authorities. Large quantities of specific secondary raw materials can be utilised in AAMs as solid binders of performance comparable to Portland cement (Ascensão et al., 2017; Bondar and Coakley, 2014; Puertas et al., 2015; Vinai et al., 2016). For new forms of concrete, the use of AAMs incorporating industrial residues reduces CO_2 emissions by up to 80% (Aiken et al., 2017). Although economically viable, market uptake and widespread application of these new types of recycled materials are currently hampered by public health concerns related to immobilisation of potentially toxic compounds (Sas and Vandevenne, 2015) and in particular radiation exposure from naturally occurring radionuclides (NORs) that can be present in these materials (Kovacs et al., 2017).

With existing construction materials and raw materials, the contents of NOR (U-238, Th-232 series and their progenies, K-40) and their effects can have significant health implications. Despite the relatively low NOR contents generally found in buildings, the radionuclides present can cause long-term exposure to the inhabitants, due to prolonged indoor residence times. Two main exposure pathways can be differentiated when considering the built environment. The primary pathway leading to internal exposure is as a result of the decay of the incorporated radionuclides from the U-238 and Th-232 decay series that leads to the formation of radon & thoron. The exposure factor, related to this pathway, is the inhalation of radon/thoron (Rn-222, Rn-220) and their progenies (from soil and construction materials) which can get stuck in the lungs and irradiate cells. Radon, a radioactive noble gas, can diffuse out of the building materials and is currently

the second most common cause of lung cancer after smoking (Axelsson et al., 2015; World Health Organization, 2009). Depending on the internal structure and the parent element concentration (Ra-226), the amount of radon which can exhale from a given building material matrix can vary greatly. The secondary pathway, the external exposure caused mainly by gamma radiation emitted from the decay of NOR also needs to be considered. Owing to their high penetration capacity, high energy gamma photons can exit walls, floors, and ceilings that contain NOR materials. This depends on several factors including the energy of the gamma photons, the thickness of the walls, the material density, the homogeneity and concentration of the radionuclides. A constant dose rate is formed as a result of the NORs in buildings. The gamma exposure can also depend on the position of the residents within rooms, but typically to a small extent (International Atomic Energy Agency, 2012; Risica et al., 2001). Screening of potential industrial residues prior to recycling ensures the avoidance of recycled building materials with increased radioactivity, and, in this way, the industrial residue streams for the circular economy are checked in advance to assure safe recycling (Kovacs et al., 2017).

To avoid an elevated risk for residents in houses, the EU has laid down Council Directive 2013/59/Euratom (European Union, 2014) as Basic Safety Standards (EU-BSS) for protection against the dangers arising from exposure to ionising radiation. Annex VIII of the directive defines the requirement for maximum allowable excess dose from the NOR contents of building materials. Furthermore, the reference level for indoor radon was set at 300 Bq/m^3 average radon concentration. However, uniform requirements and a standardised method for screening the radon release from building materials before they are placed on the market are still missing, which presents a significant challenge for future research. The NOR contents of construction materials, their raw materials and residues depend on the origin of the materials. The processing technology can also lead to a strong fluctuation in the NOR concentration, even in the case of the same residue repository (Croymans et al., 2017b).

Table 1 presents global information about the NOR contents of BA, FA, GGBFS, HWA and RM based on the NORM4Building (Schroeyers et al., 2018) and By-BM (By-Products for Building Materials) (Sas et al.,

2017) NOR databases. In relation to the other residues that this article considers, namely APC, CKD, ISSA, RHA, there are no records yet in the NOR databases (Sas, 2017; Sas et al., 2017; Schroeyers et al., 2018).

Table 1: Naturally occurring radionuclide (NOR) contents (Bq/kg) of studied residues according to NORM4Building and By-BM databases

Material	Database	Ra-226			Th-232			K-40		
		Min	Max	Average	Min	Max	Average	Min	Max	Average
BA	By-BM	16	3152	845	11	290	845	7	1100	253
FA	NORM4B	11	1000	188	1	200	91	17	1100	343
	By-BM	14	1028	235	1	250	96	44	3001	505
GGBFS	NORM4B	100	323	201	25	148	66	158	500	298
	By-BM	8	399	183	3	330	83	7	388	162
HWA	By-BM	11	25	18	8	21	13	159	213	83
RM	NORM4B	97	1700	389	45	1800	553	15	583	216
	By-BM	97	1047	311	118	1350	324	5	583	155

There is a fundamental difference between the two NOR databases. The By-BM database operates with individually reported sample information, including information on how the samples were measured, which enables further statistical analysis of the data. The disadvantage of this dataset is that it operates with a limited amount of records (currently a few thousand). The dataset contains the number of the samples with the minimum, maximum, and the average or median activity concentrations of samples. The NORM4Building dataset has a greater number of records but consists mainly of averaged data. This type of information does not allow the precise weighting of the data, but the great number of entries provides an overall insight into the materials.

Here we evaluate new radiological and chemical analysis of residues or secondary raw materials commonly used in the manufacture of alkali-activated materials by determination of NOR contents by gamma spectrometry and calculation of I-index and radium equivalent. We investigate radioactive disequilibrium in the radioactive decay chain of Th-232 and U-238 and determine massic exhalation and radon emanation factor for the residues.

2. Materials and methods

2.1 Sample preparation

Samples were collected from different European countries and originate from various industrial activities (Table 2). The sources of the samples are not revealed, as the present scientific research is not for judging them. The samples were homogeneous within each source, represented by a unique Sample ID in Table 2. FA 7 was originated from the same site as FA 1 and GGBFS 2 came from the same site as GGBFS 1. This is the reason why FA 7 and GGBFS 2 were not examined with XRF. Fig. 1 gives exact compositions of all these sample materials. All ashes are siliceous. Note that the data shown in Table 1 are from literature data forming the two databases, while the samples listed in Table 2 are for the original experimental studies, the results of which are reported in this paper. The samples were dried to constant mass in a drying cabinet at a temperature of 105°C and powdered. A typical sample weight used for subsequent analysis post drying was 1 kg. The powdered samples were divided to three portions. For the gamma spectrometry analysis and the radon exhalation measurement, typically 0.3–0.5 kg samples were used respectively depending on their density. For the XRF characterization 10 g samples were used.

Table 2: Identifier (ID) of surveyed materials

Sample ID	Material	Industry
APC	Air pollution control residue	Municipal waste incineration
BA	Bottom ash	Coal combustion thermal power plant
CKD 1, 2, 3	Cement kiln dust	Cement production
FA 1, 2, 3, 4, 5, 6, 7	Fly ash	Coal combustion thermal power plant
GGBFS 1, 2	Ground granulated blast-furnace slag	Ferrous industry
HWA	Household waste ash	Municipal waste incineration
ISSA	Incinerated sewage sludge ash	Sewage sludge incineration
RHA	Rice husk ash	Rice milling industry
RM 1, 2	Red mud	Aluminum production

2.2 Determination of major components with XRF

In this study, the main chemical composition was determined by X-ray fluorescence (XRF) analysis. The measurements were performed on a fused glass bead sample, for removing both grain size and mineralogical effects. The samples were heated under air atmosphere up to 1200°C in a platinum crucible with lithium borates. During the process, oxides of the metal contents are formed and the results are reported in that form. The equipment used was a PANalytical Axios Advanced XRF spectrometer which runs on a 4KW Rh tube using WDS and a sample to flux ratio of 1:10. The results, which were quoted as weight percent, were analysed using PANalytical SuperQ software using reference samples and artificial analogues. LOI was determined by igniting the materials at 950°C for 1.5 hours.

2.3 Determination of NOR with gamma spectrometry

The samples were put into polystyrene containers with metal cap and stored for 27 days to achieve secular equilibrium between Ra-226 and Rn-222. The NOR contents of the investigated materials were determined

by gamma spectrometry using a calibrated high purity broad energy germanium detector (Canberra BE5025-7500SL) with a 50% nominal relative efficiency. The detector was shielded with a copper-lined lead shield specific for low-activity measurements. All samples were measured for 80 000 s using the same poly(methyl methacrylate) sample holder to fix the samples in position 5 mm above the endcap of the detector, leaving an air-filled gap between the sample and the detector. Canberra's Genie 2000 software was used for data acquisition. Canberra's LabSOCS software was used to perform the efficiency calibration with self-absorption correction. The 1 sigma error was calculated by the sofware. The determined radionuclides and their details are presented in Table 3.

Table 3: Details of radionuclides measured by gamma spectrometry

Nuclide	Decay chain	Determined isotope	Energy (keV)	Intensity (%)
Pb-214	U-238	Ra-226	351.9	35.6
Bi-214	U-238	Ra-226	609.3	45.5
Th-234	U-238	U-238	63.3	3.8
Pb-210	U-238	Pb-210	46.5	4.3
Ac-228	Th-232	Th-232	911.2	26.2
Pb-212	Th-232	Th-232	238.6	43.6
K-40	-	K-40	1460.8	10.6
Cs-137	-	Cs-137	661.7	85.0

2.4 Calculation of commonly used indexes

2.4.1 Radium equivalent index

The radium equivalent index (Ra_{eq}) (Beretka and Mathew, 1985) is based on the assumption that the dose rate contribution of unit activity of Ra-226, Th-232 and K-40 with their belongings decay chains are

different. The dose criterion in the case of Ra_{eq} is 1.5 mGy/year absorbed dose which corresponds to a value of 1.0 mSv annual effective dose. The calculation of Ra_{eq} assumes that 259 Bq/kg of Th-232 and 4810 Bq/kg of K-40 cause a dose rate equivalent to 370 Bq/kg of Ra-226 (Beretka and Mathew, 1985; Nuccetelli et al., 2017). The Ra_{eq} can be calculated according to the following equation:

$$Ra_{eq} = A_{Ra-226} + 1.43 A_{Th-232} + 0.077 A_{K-40} \quad (1)$$

where $A_{Ra\text{-}226}$, $A_{Th\text{-}232}$, and $A_{K\text{-}40}$ are the activity concentration of Ra-226, Th-232, and K-40, respectively. The current Chinese and Russian legislation is derived from this approach (Nuccetelli et al., 2017).

2.4.2 Activity concentration index (I-index)

To characterise construction materials the calculation of the I-index is one of the most commonly used screening tool based on the Mikka Markannens model, presented in RP112 (European Commission, 1999). The I-index is derived to indicate whether the annual dose due to the excess external gamma radiation in a building may exceed 1.0 mSv. This calculation method operates with the assumption that all the walls, the ceiling and also the floor of the room are made from 20 cm thick concrete with 2350 kg/m^3 density. The computation considers the occupancy factor, the annual indoor spent time, and the dose conversion factor. The targeted 1.0 mSv dose excess can be the result of exposure to respectively 276 Bq/kg Ra-226, 231 Bq/kg Th-232 or 3176 Bq/kg of K-40. In the final formula of the I-index, the values computed above are rounded to the nearest full 100 Bq/kg (Ra-226 and Th-232) or 1000 Bq/kg (K-40). The latest European Basic Safety Standard (EU-BSS) in Article 75, Annex XIII (European Union, 2014) introduces a screening index which is based on the abovementioned computation to identify building materials that are of concern from the radiological protection point of view. The I-index can be calculated according to the following formula (European Commission, 1999; Nuccetelli et al., 2017):

$$I = \frac{C_{Ra}}{300 Bq/kg} + \frac{C_{Th}}{200 Bq/kg} + \frac{C_K}{3000 Bq/kg} \quad (2)$$

where C_{Ra}, C_{Th}, C_K are the Ra-226, Th-232 and K-40 activity concentrations expressed in Bq/kg.

In the European Union, the member states were required to harmonise their national legislation according to the EU-BSS at the latest in February 2018. It is important to note that the calculation of the I-index only allows for a conservative screening. To more accurately predict the dose contribution as a result of recycled building materials in a given building, the thickness and the density also have to be taken into consideration (Nuccetelli et al., 2015). A recently published dose model (Croymans et al., 2017a) with expanded gamma lines from NORs is applicable in non-standard rooms.

2.5 Massic radon exhalation and emanation factor of surveyed samples

The massic exhalation (Friedmann et al., 2017) of surveyed samples was determined with an accumulation chamber technique. The granulated (<10 mm grain size) (Friedmann et al., 2017), dry samples were enclosed in radon-tight acrylic accumulation chambers equipped with stainless steel valves. To effectively remove the radon from the samples, including pores, the chambers were evacuated in a vacuum chamber and after purged with intensive radon-free airflow. The exhaled radon was determined with RD200 (200 cm^3 chamber volume) ionisation chamber manufactured by FTLab. Circulation was used for 10 minutes with 5 L/min flow rate. To avoid the disequilibrium of the radon and its progenies, and the contribution of thoron (Jonas et al., 2016), the first result obtained from the 60 minutes of the measurement was ignored. In the accumulation time function, the activity of the decay of the exhaled radon was corrected, and the massic exhalation was calculated according to the following formula (Sas et al., 2015b):

$$E_{Mass} = \frac{C_t \cdot V}{m \cdot t} \cdot \frac{\lambda \cdot t}{1 - e^{-\lambda t}} \quad (3)$$

where C_t = accumulated radon concentration in the measurement kit during sampling [Bq m^{-3}], E_{Mass} = massic exhalation rate [mBqkg^{-1} h^{-1}], t = accumulation time [h], V = volume of the accumulation kit [m^3], m = mass of the sample [kg], λ = decay constant of radon [h^{-1}]. Error values were derived from the sensitivity of the instrument, using information provided by manufacturer.

The emanation factors of the surveyed samples were calculated from the Ra-226 activity concentration obtained by gamma spectroscopy and the equilibrium radon concentration calculated from the massic exhalation results (International Atomic Energy Agency, 2013):

$$\varepsilon = \frac{Rn_{eq}}{C_{Ra-226}} \cdot 100 \quad (4)$$

where ε = emanation factor (%), Rn_{eq} = equilibrium radon concentration and C_{Ra-226} = Ra-226 activity concentration.

3. Results and discussion

3.1 Chemical composition of surveyed samples obtained by XRF

The main chemical compositions of the studied residues are illustrated as a heat-map in Fig. 1. Dark red represents the dominant components in the samples. The SiO_2 content was the highest with 90.8 wt% in the case of the rice husk ash sample (RHA) which fits the reported data (He et al., 2013). In the case of those fly ash and bottom ash samples, the SiO_2 ranged between 42.7-56.0 wt%, the Al_2O_3 content varied between 18.4-30.0 wt% (highest among all residues studied) and the Fe_2O_3 ranged between 4.9-18.7 wt%. The fly ash samples were all siliceous and not calcareous. The CaO content was dominant in the case of all CKD, APC and GGBFS 1 samples (32.6-49.5 wt%). In the case of both red mud samples, the composition fits well with the scientifically reported data (Wang and Liu, 2012). The most dominant components in the red mud were Fe_2O_3 (35.8-43.8 wt%, highest among all residues studied), Al_2O_3 (16.3-25.1 wt%), SiO_2 (8.6-13.8 wt%), TiO_2 (5.1-10.2 wt%, highest among all residues studied), CaO (4.5-5.6 wt%) and Na_2O (4.7-7.7 wt%) which mainly originates from the NaOH solution used in the Bayer process (Kovacs et al., 2017).

Sample ID	SiO_2	TiO_2	Al_2O_3	Fe_2O_3	MnO	MgO	CaO	K_2O	Na_2O	P_2O_5	SO_3	V_2O_5	Cr_2O_3	SrO	ZrO_2	BaO	NiO	CuO	ZnO	PbO	LOI
APC	6.43	0.79	2.59	0.73	0.08	1.05	32.59	3.55	3.20	0.85	16.38	0.01	0.03	0.05	0.01	0.06	0.00	0.07	1.78	0.05	14.40
BA	56.02	0.83	18.39	7.97	0.09	1.73	5.36	2.61	0.88	0.68	0.23	0.03	0.01	0.18	0.04	0.34	0.01	0.01	0.01	0.00	4.63
CKD 1	16.37	0.21	3.73	2.21	0.06	0.88	46.62	4.35	0.37	0.13	13.67	0.01	0.01	0.07	0.01	0.04	0.00	0.01	0.06	0.03	9.90
CKD 2	14.57	0.27	3.84	2.07	0.06	0.75	49.53	9.12	1.07	0.09	4.28	0.01	0.00	0.02	0.00	0.02	0.01	0.05	0.04	0.05	13.17
CKD 3	11.83	0.24	3.49	2.39	0.18	1.60	45.44	8.29	0.93	0.05	4.61	0.06	0.01	0.03	0.01	0.02	0.01	0.03	0.01	0.02	20.21
FA 1	50.24	0.98	25.84	11.27	0.08	1.86	3.15	2.91	0.89	0.22	0.12	0.08	0.02	0.10	0.03	0.32	0.02	0.02	0.03	0.01	3.05
FA 2	53.64	0.91	20.31	9.26	0.07	1.83	4.33	2.19	1.14	0.43	0.39	0.04	0.01	0.18	0.04	0.33	0.01	0.01	0.02	0.00	4.54
FA 3	48.70	0.98	29.97	6.99	0.07	1.45	2.80	3.26	0.66	0.68	0.58	0.05	0.02	0.14	0.04	0.42	0.03	0.03	0.02	0.01	3.97
FA 4	55.45	1.07	23.90	4.86	0.05	1.72	4.43	1.89	0.81	0.72	0.73	0.03	0.01	0.18	0.00	0.43	0.01	0.01	0.02	0.01	3.19
FA 5	55.77	0.83	19.84	5.79	0.08	2.03	4.46	2.42	1.24	0.53	0.55	0.03	0.01	0.15	0.04	0.35	0.01	0.01	0.02	0.01	5.44
FA 6	42.73	0.91	27.90	18.72	0.04	0.98	4.13	1.45	0.11	0.40	0.71	0.04	0.02	0.10	0.03	0.25	0.01	0.01	0.03	0.01	2.18
GGBFS 1	34.74	0.62	13.80	0.34	0.46	7.63	41.13	0.69	0.30	0.00	2.54	0.01	0.00	0.08	0.04	0.42	0.00	0.00	0.00	0.00	0.00
HWA	35.22	0.89	12.47	10.57	0.16	2.39	19.59	1.07	4.21	1.74	1.43	0.06	0.05	0.16	0.04	0.33	0.04	0.24	0.48	0.07	7.34
ISSA	34.19	1.26	13.53	15.02	0.19	3.46	9.21	2.36	1.25	16.98	0.31	0.02	0.03	0.05	0.03	0.23	0.02	0.10	0.33	0.02	1.46
RHA	90.78	0.07	1.16	0.71	0.14	0.54	0.78	2.00	0.08	1.28	0.04	0.00	0.00	0.00	0.01	0.07	0.00	0.00	0.01	0.00	2.59
RM 1	8.58	10.17	16.25	43.76	0.05	0.07	5.64	0.09	4.68	0.32	0.16	0.23	0.25	0.01	0.35	0.21	0.01	0.00	0.01	0.01	9.33
RM 2	13.75	5.07	25.13	35.78	0.02	0.41	4.54	0.57	7.72	0.03	0.39	0.09	0.10	0.00	0.13	0.76	0.06	0.00	0.01	0.02	5.25

Fig. 1: Main chemical components (wt%) of studied residues illustrated on a heat-map chart

3.2 NOR contents

The activity concentration values obtained with gamma spectrometry of the NOR and the Cs-137 contents are presented in Table 4. Compared to the world average of NORs in construction materials (Ra-226 = 50 Bq/kg, Th-232 = 50 Bq/ kg and K-40 = 500 Bq/kg) (European Commission, 1999), the obtained average values of the residues were 1.84, 1.8 and 1.5 times higher, respectively.

There is no easy way to compare the different materials. They are associated with different raw materials and different processes. The NOR isotopes are trace elements and their behavior depends on the processes. These materials are completely independent from each other. It is not a straightforward mechanism in general. So, the results were compared in this paper only to the records of the NORM databases. A source apportionment tool can be a first step to build a dataset to provide possibility to draw conclusion for the mechanisms.

285 **Table 4: Naturally occurring radionuclide (NOR) and Cs-137 contents of surveyed materials**

286 **where the 1 sigma error was calculated by the LabSOCS software**

ID	Ra-226	Th-232	K-40	Cs-137
APC	10±1	7±1 (min.)	1025±43	6.1±0.4
BA	113±8	68±5	623±27	-
CKD 1	15±1	11±1	1348±57	0.9±0.1
CKD 2	15±1	8±1	2712±113 (max.)	4.9±0.4
CKD 3	15±1	8±1	2631±110	3.0±0.3
FA 1	139±10	82±6	743±31	1.4±0.2
FA 2	108±7	59±4	542±23	-
FA 3	89±6	94±7	763±32	-
FA 4	115±8	98±7	482±21	-
FA 5	89±6	60±4	577±25	-
FA 6	201±14 (max.)	97±7	349±15	-
FA 7	129±9	76±5	674±29	1.3±0.1
GGBFS 1	126±9	44±3	117±6	-
GGBFS 2	129±9	47±3	122±6	-
HWA	32±2	18±1	242±11	1.4±0.1
ISSA	65±5	60±4	563±24	11±1 (max.)
RHA	6±1 (min.)	16±1	505±22	-
RM 1	186±13	452±31 (max.)	37±2 (min.)	-
RM 2	168±11	398±27	174±8	-
Average	92	90	749	2

287

In Table 4, a dash line indicates no detectable data, i.e., the measured intensity was below the detection limit. The results of different studied materials were compared with the similar material records in the NORM4Building (Schroeyers et al., 2018) and By-BM (Sas et al., 2017) NOR databases. The result of the comparison is illustrated in Fig. 2.

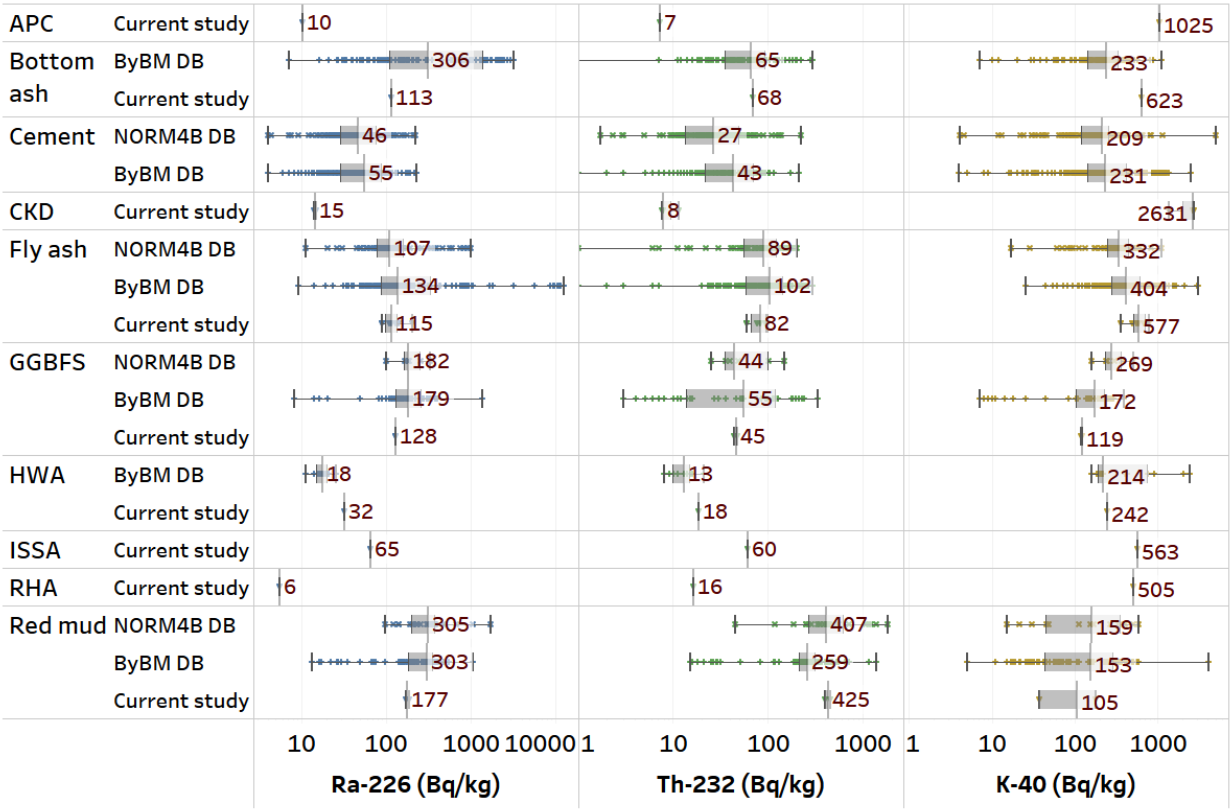

Fig. 2: Comparison of obtained naturally occurring radionuclide (NOR) contents with datasets of NOR databases with the distribution of the data and the computed average values all illustrated

Regarding APC, CKD, ISSA and RHA samples, a comparison was not possible because there was no information about these materials in either database. In the case of the other surveyed residues, their NOR contents were lower than the averages in the databases except that all three investigated NOR of the HWA, the K-40 contents of the bottom ash and fly ash samples and the Th-232 contents of the red mud were found above the average values. However, since there was no information about the CKD in the databases, the obtained results were compared with the cement records. In the case of the CKD results, the Ra-226 and

Th-232 contents were significantly lower than the average values of the cement records collected in the databases. The K-40 contents were significantly higher compared to the database records.

3.3 I-index and radium equivalent concentration of studied residues

The I-index and the radium equivalent concentration were calculated based on the obtained NOR content. However, this calculation provides only a conservative screening value, since neither the density nor the thickness of the construction materials are taken into consideration. The results are illustrated in Fig. 3.

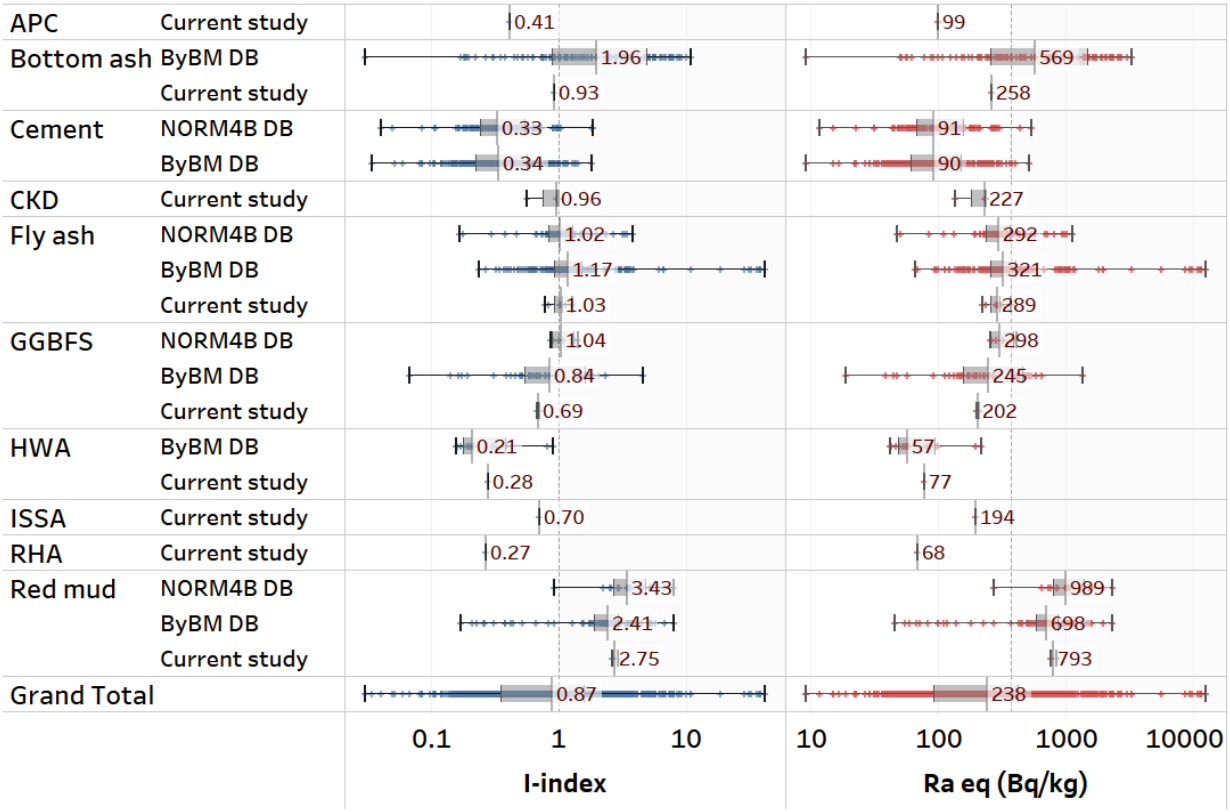

Fig. 3: Activity concentration index (I-index) and radium equivalent index (Ra_{eq}) concentration of surveyed residues compared with naturally occurring radionuclide (NOR) datasets

The I-index values varied between 0.27-2.89 with an average of 1.00. The I-index of five siliceous fly-ash and two red mud samples were found with above the EU recommended 1.0 I-index value (European Union, 2014). The Ra_{eq} concentration of the residues was lower than 370 Bq/kg for all cases, except the red mud samples. However, the Ra_{eq} concentration seems to be considerably more permissive compared to the I-

index: it has to be highlighted that 370 Bq/kg Ra_{eq} concentration is equivalent to 1.2 times the I-index value which is about 20% higher than the I-index recommended value of 1.0. In the case of the I-index, the targeted excess external dose from the building materials is 1.0 mSv/a. The dose contribution of the ICRP 115 (Tirmarche et al., 2010) and EU-BSS (European Union, 2014) recommended 300 Bq/kg average radon concentration which corresponds to approximately 10 mSv/year effective dose (Paquet et al., 2017). Clearly, the acceptable excess dose from the gamma exposure is significantly lower relative to the acceptable radon exposure. The comparison of the calculated values is presented in Fig. 4. The trendline was placed with its 95% confidence bands to represent the uncertainty in an estimate of a curve or function based on limited or noisy data. As confidence intervals are constructed and only refer to a single point, they are narrower (at this point) than a confidence band which is supposed to hold simultaneously at many points (Härdle et al., 2004).

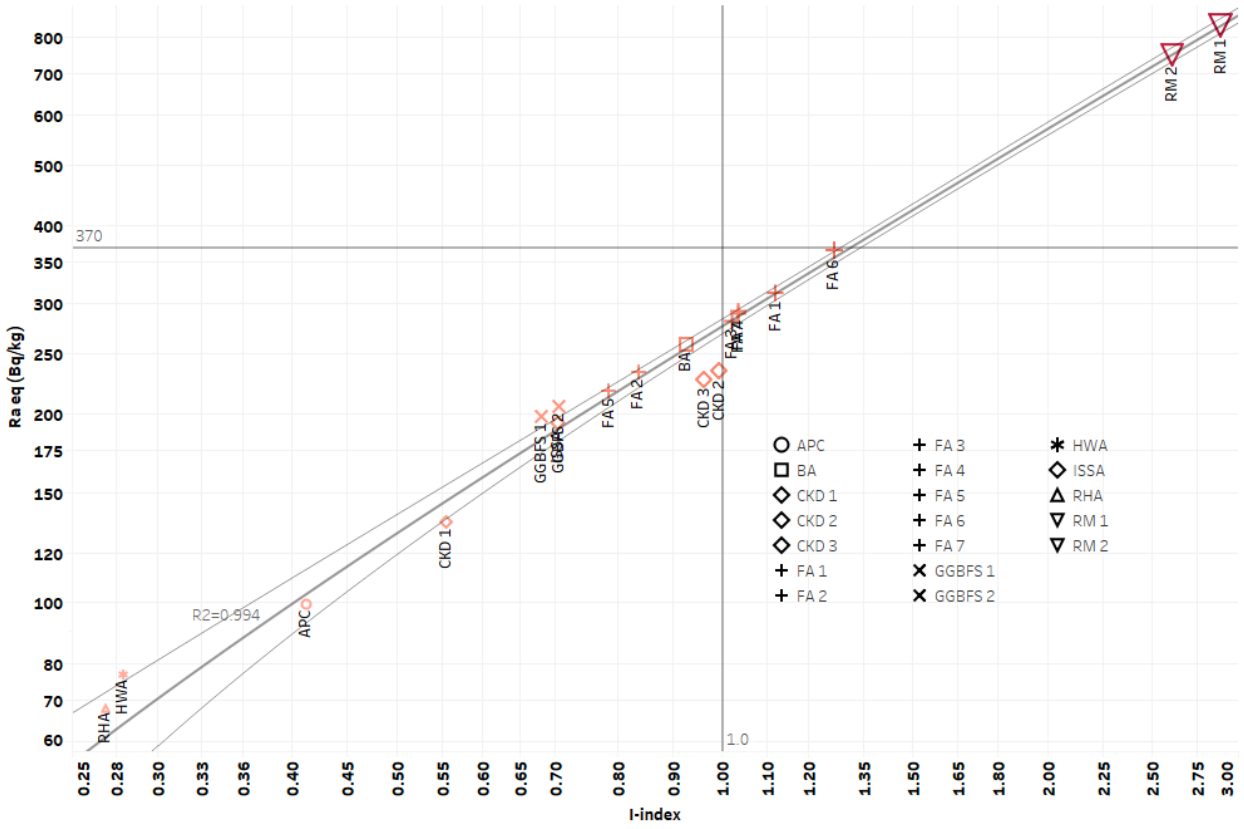

Fig. 4: Relationship between the calculated I-indexes and radium equivalent concentrations of studied residues with 95% confidence bands

However, certain samples do not fulfil the criteria of I-index. It has to be noted that both the Ra_{eq} and the I-index are used for only screening of construction materials. Individually, none of the studied residues are suitable for direct use as a 100% building material. This means the final I-index and the Ra_{eq} of any building material that contains a proportion of these residues have to be calculated to incorporate the residues and other components of any building material based on their total NOR contents (Sas et al., 2017; Schroeyers et al., 2018). According to the databases, the aggregates and the cement used for concrete production have significantly lower NOR contents resulting in a lower I-index. The mixing of the industrial residues with other construction material components (aggregates/cements) dilutes the NOR contents and allows the final NOR contents of the recycled construction materials to be under levels defined by different national legislation (Sas et al., 2015a; Nuccetelli et al., 2017).

3.4 Radioactive equilibrium of U-238 and Th-232 decay chains of the studied industrial residues

The radioactive equilibrium state of U-238 decay chain was investigated. The U-238 content was obtained from the Th-234 content (63.3 keV gamma line) of the studied samples. The Pb-210 activity concentrations were obtained via the 46.5 keV gamma peak. To check the equilibrium condition in the chain, the Ra-226 activity concentrations were used as a reference value. However, in the case of the Th-232 chain, the most significant possibility for disequilibrium may occur between the Th-232 and Ra-228 owing to the 5.74 years half-life of Ra-228. Since direct measurement of Th-232 via gamma and alpha spectrometry was not possible, its content was not determined. There was no information about the date when the residues were generated so exact age of the samples was also not known. Owing to these facts, the disequilibrium state was not investigated in the case of Th-232 chain. The disequilibrium state of U-238 chain related to Ra-226 content is presented in Fig. 5.

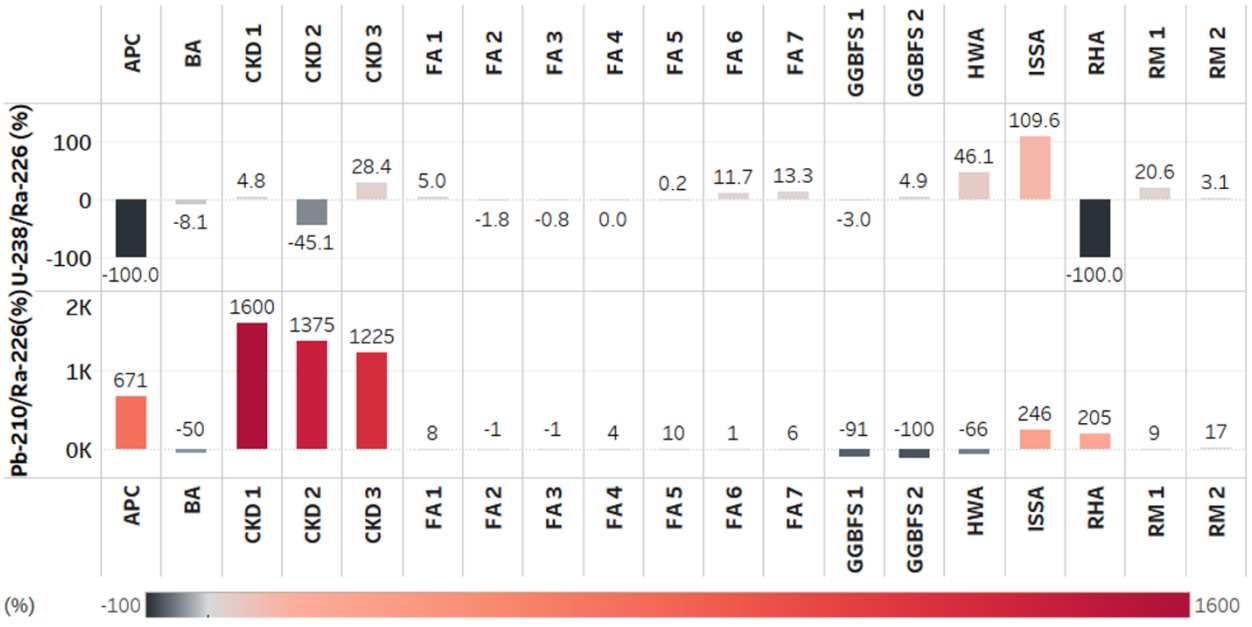

Fig. 5: Equilibrium state of U-238 decay chain related to Ra-226 content

The calculated values showed that the U-238 disappeared in the case APC and the RHA samples and in the case of CKD 2 the U-238 content was 45.1% lower compared to Ra-226 activity concentration. The disequilibrium state of RHA suggests that the uranium uptake or bioaccumulation by the rice from soil is extremely low. Significant U-238 enhancement was found in the case of HWA and ISSA samples. Both samples originate as a result of incineration of materials containing significant amounts of various organic compounds. Pb and the Po are relatively volatile elements in high-temperature combustion environments as is the case for coal combustion, cement production, and incineration of wastes. In this study, all the samples are generated from high-temperature treatment, except for red mud, which is produced by the Bayer-process. Owing to the high temperature, the volatile radionuclides condensate on the fine ash particles (Ozden et al., 2018) which can result in elevated levels of Pb-210 in the fly ash type residues with decreased levels in the bottom ash residues. The bottom ash residues, the BA, and both GGBFS and HWA samples had significantly lower Pb-210 content compared to their Ra-226 content. The fine ash type residues had significantly increased Pb-210 content compared to Ra-226 except for all FA samples. The Pb-210 content of all CKD samples was extremely high with 13-16 times higher Pb-210 content compared to the Ra-226 activity concentration. This can be explained by the condensation of these isotopes in the kiln during the cooling

phase of operation and their subsequent release during preheating when the CKD accumulates these isotopes. However, the exact mechanism should be investigated in more detail in future research projects. The APC, ISSA and RHA samples had also increased Pb-210 content with a factor of 6.7, 2.5 and 2.1, respectively, which fits with the conclusion based on the volatility of Pb and Po. The FA samples did not show significant Pb-210 accumulation which is not unusual in the case of FA residues. Relatively low enrichment factors can also be found in the literature (Ozden et al., 2018).

3.5 Correlation between NOR contents and chemical composition

The correlation between the NOR isotopes and the chemical composition results is presented in Fig. 6. In the figure, the dark colours indicate the strong correlation between the NOR isotopes and the chemical composition data. From the results it can be concluded that the Ra-226 concentration has a strong positive correlation with the Al_2O_3, BaO and Fe_2O_3 contents and strong negative correlation was found with the K_2O content. In the case of Th-232, the Cr_2O_3, Fe_2O_3, Na_2O, TiO_2, V_2O_5 and ZrO_2 contents had strong positive correlation with Th-232. The K-40 content showed strong correlation with the CaO and, of course, with the K_2O content. Strong negative correlation was found when compared with the BaO content. No correlation with the P_2O_5 content was observed for any of the NORs. Owing to the various industrial processes and the results of the heat map, it can be concluded that the NOR isotope contents can be expected to correlate with the oxides mentioned above.

Fig. 6: Comparison between the naturally occurring radionuclide (NOR) isotopes and main chemical compositions illustrated on a heat-map type diagram

The purpose of the correlation analysis was to examine the possibility of using the information about the chemical composition as a source apportionment tool for NORs. This is useful considering the future recovery of materials from old landfills, lagoons, or illegal dumps where information on the original material is not available. Based on the Pearson correlation results, the strong correlation, either positive or negative, shows that the concept is promising to predict the level of the expected NOR content. However, the conclusion was drawn from 19 samples, so the extension of the dataset and further correlation analysis could strengthen the concept.

3.6 Radon emanation and massic exhalation features of the studied samples

After the gamma spectrometry measurements, the massic radon exhalation of the samples was determined, and their radon emanation factor was calculated with the obtained Ra-226 content. The obtained results are illustrated in Fig. 7. The massic exhalation of the residues varied between 0.7 $mBqkg^{-1}h^{-1}$ and 121.0 $mBqkg^{-1}h^{-1}$ with an average of 16.1 $mBqkg^{-1}h^{-1}$. The emanation factor was obtained between 0.6-8.6%. The average of the emanation factor was 2.7%. This variation of the emanation factor of certain materials can be explained by the different emanation coefficients, which depends on the characteristic of the material matrix (Hegedus et al., 2016; Kovacs et al., 2016; Sas et al., 2015b). The results generally match those reported in various publications (International Atomic Energy Agency, 2013). The two highest massic exhalation rates

were found in the case of the red mud samples which can be explained by their significantly higher Ra-226 content and their relatively high emanation coefficient. In the case of the fly ash samples, seven samples were analysed from different origins. The calculated emanation factors were under 2% in all the seven cases which fit well with the literature data (International Atomic Energy Agency, 2013; Sas et al., 2014).

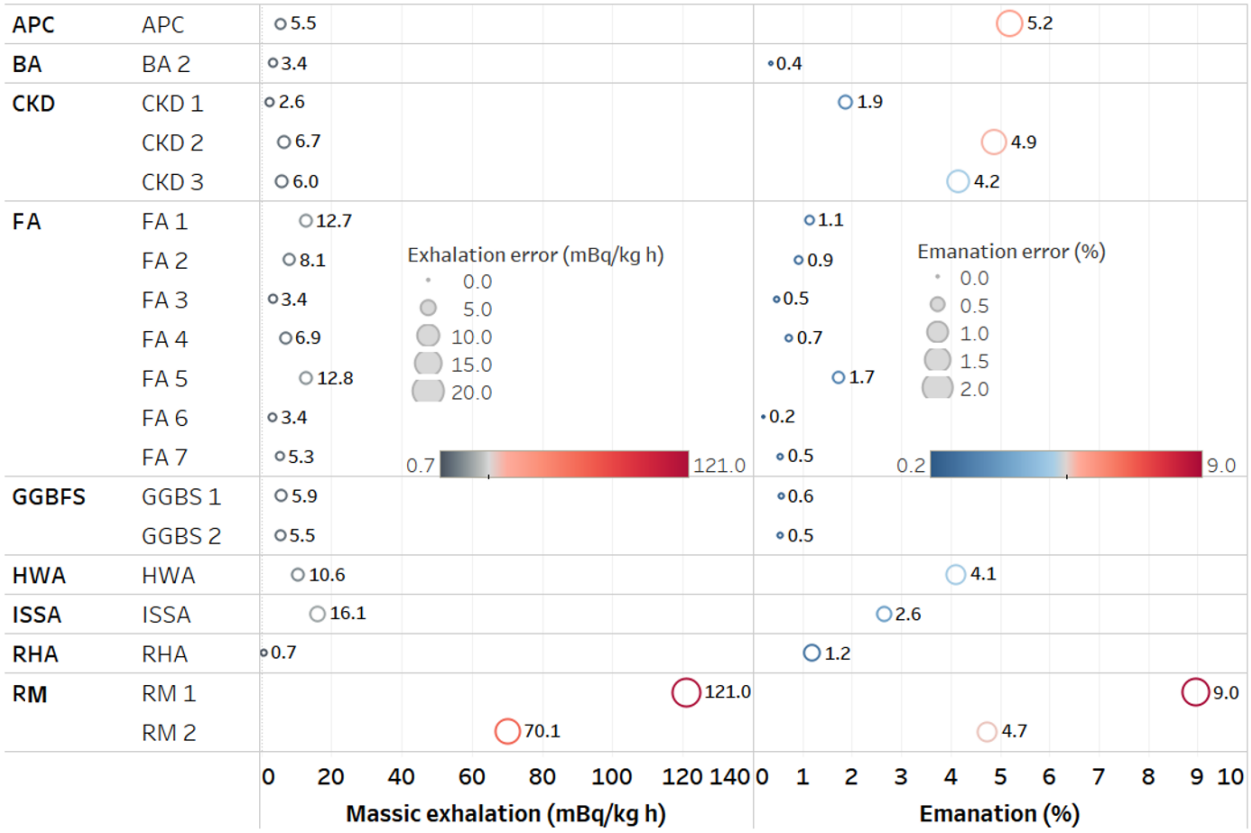

Fig. 7: Massic exhalation and emanation factor of studied samples, where the error values were derived from the sensitivity of the instrument, using information provided by manufacturer

The massic radon exhalation depends on the Ra-226 content and the emanation factor of the matrix (International Atomic Energy Agency, 2013). That is why the belonging values and their correlation were also investigated. The results of the comparison are illustrated in Fig. 8.

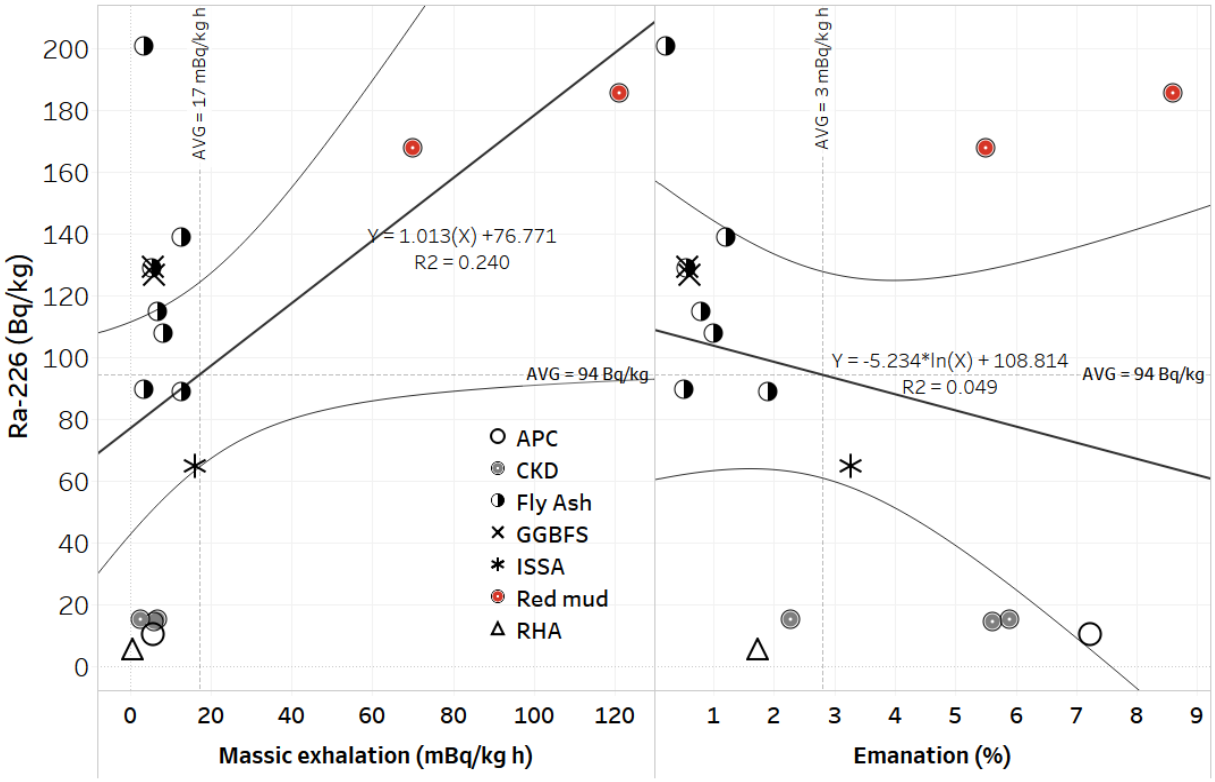

Fig. 8: Correlation between the Ra-226 and massic exhalation results and Ra-226 and emanation factor with 95% confidence bands

However, during the analysis, the fitting of a linear trendline showed a weak correlation between the Ra-226 and the massic exhalation. The relatively low number of the samples does not make possible to state the relationship between these parameters explicitly. Furthermore, the emanation factor also influences the massic exhalation. Between the Ra-226 and the emanation factor no correlation was found which proves that they are independent parameters. Measuring the Ra-226 content by itself does not allow an assessment to verify whether the radon exhalation of building materials is increased or reduced.

4. Conclusions

From the results, there were no extraordinary NOR contents in the case of any of the samples. Compared with recently published NOR databases the values were close to the average values of the datasets. The

highest NOR contents were found in the case of the red mud samples which emphasize the importance of the detemination of its NOR contents before reusing it for construction material purposes.

The radioactive equilibrium state in the decay chains fits well with the scientifically reported data. In the case of all the cement kiln dust, 13-16 times higher Pb-210 content compared to the Ra-226 activity concentration was observed which requires further investigation to find out the exact reason for the accumulation.

Significant positive correlation was found between the Ra-226 and the Al_2O_3, BaO and Fe_2O_3 contents and strong negative correlation were found with the K_2O content. Strong negative correlation was observed with the CaO content. Th-232 had a strong positive correlation with the Cr_2O_3, Fe_2O_3, Na_2O, TiO_2, V_2O_5 and ZrO_2 content. The K-40 content had a strong positive correlation with the CaO and the K_2O content while strong negative correlation was found with the BaO content.

The massic exhalation demonstrated a broad range. The highest values were found in the case of the red mud samples. The emanation coefficients were significantly lower in the case of the residues generated as a result of high-temperature processes. Compared with literature data (International Atomic Energy Agency, 2013), all the obtained emanation factors are regular.

These emanation coefficients, chemical correlations together with the radioactive equilibrium state could be used to source apportion materials found during the process of landfill mining and recovery of material for recycling, by, for example, mixing more active materials with less active materials to achieve an overall acceptable mix from the radioactivity point of view.

Acknowledgements

The project leading to this paper has received funding from the European Union's Horizon 2020 research and innovation programme under the Marie Sklodowska-Curie grant agreement No 701932. R. Doherty's time was also supported by the European Union's Horizon 2020 research and innovation programme under

the Marie Sklodowska-Curie grant agreement No 643087. The authors would also like to acknowledge networking support by the COST Action TU1301 (www.norm4building.org).

References

Aiken, T.A., Sha, W., Kwasny, J., Soutsos, M.N., 2017. Resistance of geopolymer and Portland cement based systems to silage effluent attack. Cem. Concr. Res. 92, 56–65. https://doi.org/10.1016/j.cemconres.2016.11.015

Ascensão, G., Seabra, M.P., Aguiar, J.B., Labrincha, J.A., 2017. Red mud-based geopolymers with tailored alkali diffusion properties and pH buffering ability. J. Clean. Prod. 148, 23–30. https://doi.org/10.1016/j.jclepro.2017.01.150

Axelsson, G., Andersson, E.M., Barregard, L., 2015. Lung cancer risk from radon exposure in dwellings in Sweden: how many cases can be prevented if radon levels are lowered? Cancer Causes Control 26, 541–547. https://doi.org/10.1007/s10552-015-0531-6

Beretka, J., Mathew, P.J., 1985. Natural radioactivity of Australian building materials, industrial wastes and by-products. Health Phys. 48, 87–95. https://doi.org/10.1097/00004032-198501000-00007

Bondar, D., Coakley, E., 2014. Use of gypsum and CKD to enhance early age strength of High Volume Fly Ash (HVFA) pastes. Constr. Build. Mater. 71, 93–108. https://doi.org/10.1016/j.conbuildmat.2014.08.015

Carvalho, F.P., 2017. Can the incineration of Municipal Solid Waste pose occupational and environmental radiation hazards? Int. J. Occup. Environ. Saf. 1, 1–10. https://doi.org/10.24840/2184-0954_001.001_0001

Croymans, T., Leonardi, F., Trevisi, R., Nuccetelli, C., Schreurs, S., Schroeyers, W., 2017a. Gamma exposure from building materials – A dose model with expanded gamma lines from naturally occurring radionuclides applicable in non-standard rooms. Constr. Build. Mater. 159, 768–778. https://doi.org/10.1016/j.conbuildmat.2017.10.051

Croymans, T., Vandael Schreurs, I., Hult, M., Marissens, G., Lutter, G., Stroh, H., Schreurs, S., Schroeyers,

W., 2017b. Variation of natural radionuclides in non-ferrous fayalite slags during a one-month production period. J. Environ. Radioact. 172, 63–73. https://doi.org/10.1016/j.jenvrad.2017.03.004

Cyr, M., Coutand, M., Clastres, P., 2007. Technological and environmental behavior of sewage sludge ash (SSA) in cement-based materials. Cem. Concr. Res. 37, 1278–1289. https://doi.org/10.1016/j.cemconres.2007.04.003

Davris, P., Balomenos, E., Panias, D., Paspaliaris, I., 2015. Chapter 12 - Leaching rare earth elements from bauxite residue using brønsted acidic ionic liquids, in: De Lima, I.B., Leal Filho, W. (Eds.), Rare Earths Industry. Elsevier, pp. 183–197. https://doi.org/https://doi.org/10.1016/B978-0-12-802328-0.00012-7

Donatello, S., Cheeseman, C.R., 2013. Recycling and recovery routes for incinerated sewage sludge ash (ISSA): A review. Waste Manag. 33, 2328–2340. https://doi.org/10.1016/j.wasman.2013.05.024

European Commission, 1999. Radiological protection principles concerning the natural radioactivity of building materials, RP-112. Luxemburg.

European Commission, 2015. An EU action plan for the circular economy. Com 614, 21.

European Union, 2014. Council Directive 2013/59/Euratom of 5 December 2013 laying down basic safety standards for protection against the dangers arising from exposure to ionising radiation, and repealing Directives 89/618/Euratom, 90/641/Euratom, 96/29/Euratom, 97/43/Euratom a. Off. J. Eur. Commun. L13, 1–73. https://doi.org/10.3000/19770677.L_2014.013.eng

Friedmann, H., Nuccetelli, C., Michalik, B., Anagnostakis, M., Xhixha, G., Kovler, K., de With, G., Gascó, C., Schroeyers, W., Trevisi, R., Antropov, S., Tsapalov, A., Kunze, C., Petropoulos, N.P., 2017. Measurement of NORM, in: Naturally Occurring Radioactive Materials in Construction. Elsevier, pp. 61–133. https://doi.org/10.1016/B978-0-08-102009-8.00005-0

Gelencsér, A., Kováts, N., Turóczi, B., Rostási, Á., Hoffer, A., Imre, K., Nyiró-Kósa, I., Csákberényi-Malasics, D., Tóth, Á., Czitrovszky, A., Nagy, A., Nagy, S., Ács, A., Kovács, A., Ferincz, Á., Hartyáni, Z., Pósfai, M., 2011. The red mud accident in Ajka (Hungary): Characterization and potential health effects of fugitive dust. Environ. Sci. Technol. 45, 1608–1615. https://doi.org/10.1021/es104005r

Gunning, P.J., Hills, C.D., Carey, P.J., 2010. Accelerated carbonation treatment of industrial wastes. Waste Manag. 30, 1081–1090. https://doi.org/10.1016/j.wasman.2010.01.005

Härdle, W., Werwatz, A., Müller, M., Sperlich, S., 2004. Nonparametric Density Estimation. Springer, pp. 39–83. https://doi.org/10.1007/978-3-642-17146-8_3

He, J., Jie, Y., Zhang, J., Yu, Y., Zhang, G., 2013. Synthesis and characterization of red mud and rice husk ash-based geopolymer composites. Cem. Concr. Compos. 37, 108–118. https://doi.org/10.1016/j.cemconcomp.2012.11.010

Hegedus, M., Sas, Z., Toth-Bodrogi, E., Szanto, T., Somlai, J., Kovacs, T., 2016. Radiological characterization of clay mixed red mud in particular as regards its leaching features. J. Environ. Radioact. 162–163, 1–7. https://doi.org/10.1016/j.jenvrad.2016.05.002

International Atomic Energy Agency, 2012. Protection of the public against exposure indoors due to natural sources of radiation, IAEA Safety Standards Series. Vienna.

International Atomic Energy Agency, 2013. Measurement and calculation of radon releases from NORM residues, Technical Reports Series. Vienna.

ISCORS, 2005. Assessment of Radioactivity in Sewage Sludge: Recommendations on Management of Radioactive Materials in Sewage Sludge and Ash at Publicly Owned Treatment Works.

Jonas, J., Sas, Z., Vaupotic, J., Kocsis, E., Somlai, J., Kovacs, T., 2016. Thoron emanation and exhalation of Slovenian soils determined by a PIC detector-equipped radon monitor. Nukleonika 61, 379–384. https://doi.org/10.1515/nuka-2016-0063

Kardos, R., Sas, Z., Hegedus, M., Shahrokhi, A., Somlai, J., Kovacs, T., 2015. Radionuclide content of NORM by-products originating from the coal-fired power plant in Oroszlány (Hungary). Radiat. Prot. Dosimetry 167, 266–9. https://doi.org/10.1093/rpd/ncv259

Kourti, I., Amutha Rani, D., Deegan, D., Cheeseman, C.R., Boccaccini, A.R., 2010. Development of geopolymers from plasma vitrified air pollution control residues from energy from waste plants, in: Ceramic Transactions. John Wiley & Sons, Inc., Hoboken, NJ, USA, pp. 297–304. https://doi.org/10.1002/9780470909836.ch28

527 Kovacs, T., Shahrokhi, A., Sas, Z., Vigh, T., Somlai, J., 2016. Radon exhalation study of manganese clay
528 residue and usability in brick production. J. Environ. Radioact.
529 https://doi.org/http://dx.doi.org/10.1016/j.jenvrad.2016.07.014
530 Kovacs, T., Bator, G., Schroeyers, W., Labrincha, J., Puertas, F., Hegedus, M., Nicolaides, D., Sanjuán,
531 M.A., Krivenko, P., Grubeša, I.N., Sas, Z., Michalik, B., Anagnostakis, M., Barisic, I., Nuccetelli, C.,
532 Trevisi, R., Croymans, T., Schreurs, S., Todorović, N., Vaiciukyniene, D., Bistrickaite, R., Tkaczyk,
533 A., Kovler, K., Wiegers, R., Doherty, R., 2017. From raw materials to NORM by-products, in:
534 Naturally Occurring Radioactive Materials in Construction. Elsevier, pp. 135–182.
535 https://doi.org/10.1016/B978-0-08-102009-8.00006-2
536 Liu, K., 2016. Red mud strikes again - AZ China [WWW Document]. Black China Blog. URL http://az-
537 china.com/archives/7980# (accessed 1.12.18).
538 Mayes, W.M., Burke, I.T., Gomes, H.I., Anton, Á.D., Molnár, M., Feigl, V., Ujaczki, É., 2016. Advances
539 in understanding environmental risks of red mud after the Ajka spill, Hungary. J. Sustain. Metall. 2,
540 332–343. https://doi.org/10.1007/s40831-016-0050-z
541 Müller, U., Rübner, K., 2006. The microstructure of concrete made with municipal waste incinerator bottom
542 ash as an aggregate component. Cem. Concr. Res. 36, 1434–1443.
543 https://doi.org/10.1016/j.cemconres.2006.03.023
544 Nuccetelli, C., Leonardi, F., Trevisi, R., 2015. A new accurate and flexible index to assess the contribution
545 of building materials to indoor gamma exposure. J. Environ. Radioact. 143, 70–75.
546 https://doi.org/10.1016/j.jenvrad.2015.02.011
547 Nuccetelli, C., de With, G., Trevisi, R., Vanhoudt, N., Pepin, S., Friedmann, H., Xhixha, G., Schroeyers,
548 W., Aguiar, J., Hondros, J., Michalik, B., Kovler, K., Janssens, A., Wiegers, R., 2017. Legislative
549 aspects, in: Naturally Occurring Radioactive Materials in Construction. Elsevier, pp. 37–60.
550 https://doi.org/10.1016/B978-0-08-102009-8.00004-9
551 Olivier, J.G.J., Janssens-Maenhout, G., Muntean, M., Peters, J.A.H.W., 2016. Trends in Global CO_2
552 Emissions: 2016 Report, PBL Netherlands Environmental Assessment Agency & European

553 Commission's Joint Research Centre (JRC).
554 Ozden, B., Guler, E., Vaasma, T., Horvath, M., Kiisk, M., Kovacs, T., 2018. Enrichment of naturally
555 occurring radionuclides and trace elements in Yatagan and Yenikoy coal-fired thermal power plants,
556 Turkey. J. Environ. Radioact. 188, 100–107. https://doi.org/10.1016/j.jenvrad.2017.09.016
557 Pan, S.Y., Chiang, P.C., Pan, W., Kim, H., 2018. Advances in state-of-art valorization technologies for
558 captured CO2toward sustainable carbon cycle. Crit. Rev. Environ. Sci. Technol. 48, 471–534.
559 https://doi.org/10.1080/10643389.2018.1469943
560 Paquet, F., Bailey, M.R., Leggett, R.W., Lipsztein, J., Marsh, J., Fell, T.P., Smith, T., Nosske, D., Eckerman,
561 K.F., Berkovski, V., Blanchardon, E., Gregoratto, D., Harrison, J.D., 2017. ICRP Publication 137:
562 Occupational Intakes of Radionuclides: Part 3. Ann. ICRP 46, 1–486.
563 https://doi.org/10.1177/0146645317734963
564 Puch, K.-H., Bialucha, R., Keller, G., 2005. Naturally occurring radioactivity in industrial by-products from
565 coal-fired power plants, from municipal waste incineration and from the iron- and steel-industry, in:
566 Radioactivity in the Environment. pp. 996–1008. https://doi.org/10.1016/S1569-4860(04)07123-2
567 Puertas, F., Alonso, M.M., Torres-Carrasco, M., Rivilla, P., Gasco, C., Yagüe, L., Suárez, J.A., Navarro,
568 N., 2015. Radiological characterization of anhydrous/hydrated cements and geopolymers. Constr.
569 Build. Mater. 101, 1105–1112. https://doi.org/10.1016/j.conbuildmat.2015.10.074
570 Rani, D.A., Boccaccini, A.R., Deegan, D., Cheeseman, C.R., 2008. Air pollution control residues from
571 waste incineration: Current UK situation and assessment of alternative technologies. Waste Manage.
572 28, 2279–2292. https://doi.org/10.1016/j.wasman.2007.10.007
573 Risica, S., Bolzan, C., Nuccetelli, C., 2001. Radioactivity in building materials: room model analysis and
574 experimental methods. Sci. Total Environ. 272, 119–126. https://doi.org/10.1016/S0048-
575 9697(01)00675-1
576 Sas, Z., Kardos, R., Szanto, J., Shahrokhi, A., Somlai, J., Kovacs, T., 2014. Natural radionuclide content of
577 NORM by-products originated from coal fired power plant. The 9th International Symposium on the
578 Natural Radiation Environment (NRE-IX) Hirosaki, Japan.

579 Sas, Z., Vandevenne, N., 2015. Radiological aspects of the reuse of red mud as a construction material
580 additive – industrially useful characterization options, COST Action TU1301 NORM4Building
581 Workshop: Residue valorization in construction materials considering chemical and radiologica.
582 Sas, Z., Somlai, J., Szeiler, G., Kovacs, T., 2015a. Usability of clay mixed red mud in Hungarian building
583 material production industry. J. Radioanal. Nucl. Chem. 306, 271–275.
584 https://doi.org/10.1007/s10967-015-3966-z
585 Sas, Z., Szanto, J., Kovacs, J., Somlai, J., Kovacs, T., 2015b. Influencing effect of heat-treatment on radon
586 emanation and exhalation characteristic of red mud. J. Environ. Radioact. 148, 27–32.
587 https://doi.org/10.1016/j.jenvrad.2015.06.002
588 Sas, Z., Doherty, R., Kovacs, T., Soutsos, M., Sha, W., Schroeyers, W., 2017. Radiological evaluation of
589 by-products used in construction and alternative applications; Part I. Preparation of a natural
590 radioactivity database. Constr. Build. Mater. 150, 227–237.
591 https://doi.org/10.1016/j.conbuildmat.2017.05.167
592 Schroeyers, W., Sas, Z., Bator, G., Trevisi, R., Nuccetelli, C., Leonardi, F., Schreurs, S., Kovacs, T., 2018.
593 The NORM4Building database, a tool for radiological assessment when using by-products in building
594 materials. Constr. Build. Mater. 159, 755–767. https://doi.org/10.1016/j.conbuildmat.2017.11.037
595 Somlai, J., Kanyar, B., Bodnar, R., Nemeth, C., Lendvai, Z., 1996. Radiation dose contribution from coal-
596 slags used as structural building material. J. Radioanal. Nucl. Chem. Artic. 207, 437–443.
597 https://doi.org/10.1007/BF02071248
598 Somlai, J., Jobbagy, V., Nemeth, C., Gorjanacz, Z., Kavasi, N., Kovacs, T., 2006. Radiation dose from coal
599 slag used as building material in the Transdanubian region of Hungary. Radiat. Prot. Dosimetry 118,
600 82–87. https://doi.org/10.1093/rpd/nci323
601 Somlai, J., Kovacs, J., Sas, Z., Bui, P., Szeiler, G., Jobbagy, V., Kovacs, T., 2010. Vörösiszap-tározó
602 sérülésével kapcsolatos sugárterhelés becslése. Magy. Kémikusok Lapja 378–379.
603 Tirmarche, M., Harrison, J.D., Laurier, D., Paquet, F., Blanchardon, E., Marsh, J.W., 2010. Lung Cancer
604 Risk from Radon and Progeny and Statement on Radon. Ann. ICRP 40, 1–64.

https://doi.org/10.1016/j.icrp.2011.08.011

Tong, K.T., Vinai, R., Soutsos, M.N., 2018. Use of Vietnamese rice husk ash for the production of sodium silicate as the activator for alkali-activated binders. J. Clean. Prod. 201, 272–286. https://doi.org/10.1016/j.jclepro.2018.08.025

US EPA, 2016. Cement kiln dust waste [WWW Document]. Wastes - Non-Hazardous Waste - Ind. Waste. URL https://archive.epa.gov/epawaste/nonhaz/industrial/special/web/html/index-2.html (accessed 12.7.17).

Vinai, R., Rafeet, A., Soutsos, M., Sha, W., 2016. The role of water content and paste proportion on physico-mechanical properties of alkali activated fly ash GGBS concrete. J. Sustain. Metall. 2, 51–61. https://doi.org/10.1007/s40831-015-0032-6

Wang, P., Liu, D., 2012. Physical and chemical properties of sintering red mud and Bayer red mud and the implications for beneficial utilization. Materials 5, 1800–1810. https://doi.org/10.3390/ma5101800

Wongsa, A., Boonserm, K., Waisurasingha, C., Sata, V., Chindaprasirt, P., 2017. Use of municipal solid waste incinerator (MSWI) bottom ash in high calcium fly ash geopolymer matrix. J. Clean. Prod. 148, 49–59. https://doi.org/10.1016/j.jclepro.2017.01.147

World Health Organization, 2009. WHO Handbook on indoor radon: A public health perspective. Geneva. https://doi.org/10.1080/00207230903556771